Available online at www.sciencedirect.com
SCIENCE DIRECT
ELSEVIER
Tectonophysics 412 (2006) 141–157
TECTONOPHYSICS
www.elsevier.com/locate/tecto

Explosion seismic P and S velocity and attenuation constraints on the lower crust of the North–Central Tibetan Plateau, and comparison with the Tethyan Himalayas: Implications on composition, mineralogy, temperature, and tectonic evolution

A. Galvé [a,b,*], M. Jiang [c], A. Hirn [a], M. Sapin [a], M. Laigle [a], B. de Voogd [d], J. Gallart [e], H. Qian [c]

[a] *Laboratoire de Sismologie Expérimentale, Dpt. de Sismologie UMR 7580 CNRS, Institut de Physique du Globe de Paris, 4 place Jussieu, 75252 Paris Cedex 05, France*
[b] *School of Earth Sciences, Victoria University of Wellington, P.O. Box 600, Wellington, New Zealand*
[c] *Continental Dynamics Lab., Geological Institute, Chinese Academy of Geosciences, Baiwanzhuang road, 100037 Beijing, China*
[d] *Dpt Sciences de la Terre, MIGP UMR 5212, Université de Pau, 64000 Pau, France*
[e] *Institute of Earth Sciences Jaume Almera, Consejo Superior de Investigaciones Cientificas, calle Lluis Sole i Sabaris, Barcelona 08028, Spain*

Received 14 September 2004; received in revised form 9 September 2005; accepted 26 September 2005
Available online 1 December 2005

Abstract

P and S velocity and attenuation estimates in the lower crust are obtained from a set of wide angle reflection–refraction profiles in the region of active tectonics at the NE edge of the Tibetan Plateau and discussed together with respect to similar data at its Himalaya–south Tibet edge.

The quality factor is estimated in the lower half of the crust by accounting for the differential effect on amplitude–frequency observed between waves of different penetrations, and both in P and S modes. Attenuation values allow to exclude a significant proportion of partial melt and to estimate the homologous temperature, ratio of in situ to solidus absolute temperatures. The latter depend on the physical conditions being of dry, wet or dehydration melting, which are found different among the regions of the northern Bayan Har and northern Qang Tang boundaries between blocks, as well as the Tethyan–Himalayas, south of the Indus–Tsangpo suture. Their in situ temperatures differ also as estimated from their different V_p for a similar felsic composition.

Joint measurement of several parameters, V_p, V_s, Q_p and Q_s reveals the composition, mineralogy, temperature and hydration conditions of the lower half of the thickened crust of Tibet that may be discussed in terms of evolution. The material presently in the thickened crust, even its lower part, has a felsic composition, upper to middle crustal lithology, and the temperature conditions estimated suggest that basic material that could have underlain it could be eclogitized and not appear anymore above the seismic Moho.

Under northern Qang Tang, the felsic material in the lower half of the crust appears as hot and dry. Its burial may have occurred earlier or may have been moderate in the postcollisional phase. This is consistent with a model of indentation of the Qang Tang crust by an originally thinner Bayan Har crust to bring part of its crust to greater depth, suggested from imaging the crustal architecture. Under northern Bayan Har, the material in the lower half of the crust appears as felsic, at low temperature and not dry

* Corresponding author. Dpt Sismologie, Case 89, Institut de Physique du Globe, de Paris, 4, Place Jussieu, 75252 Paris Cedex 05, France. Tel.: +33 1 44 27 39 14; fax: +33 1 44 27.
E-mail address: GALVE@IPGP.JUSSIEU.FR (A. Galvé).

0040-1951/$ - see front matter
doi:10.1016/j.tecto.2005.09.010

conditions. This is evidence that it has been transported from a shallower depth, and this recently enough not to be yet dehydrated and temperature equilibrated in a conductive geotherm. It supports a model of recent overriding of the middle crust of the north Kun Lun block to the north independently suggested from the image of crustal architecture. The Tethyan Himalayas case appears bracketed by these two cases in northern Tibet for V_p and temperature conditions, but shows highest attenuation in the lower crust that is colder but less dry than under northern Qang Tang.

Keywords: Tibet; Explosion seismology; Seismic velocity; Seismic attenuation; Crustal structure; Composition

1. Introduction

Attenuation is often not discussed in seismic studies of the crust and lithosphere since its effect may not be obvious or there may not be likely causes for it being significant. The case may be different in Tibet, since early on Bird and Toksöz (1977) derived significant attenuation of surface wave from 20-s Rayleigh waves, which they represented by an S-attenuation thickness of 2 km centred at the 70 km depth of the crust–mantle boundary. That is an attenuation of magnitude equivalent to that of a 2 km thick layer of $Q_s = 1$. If half of this

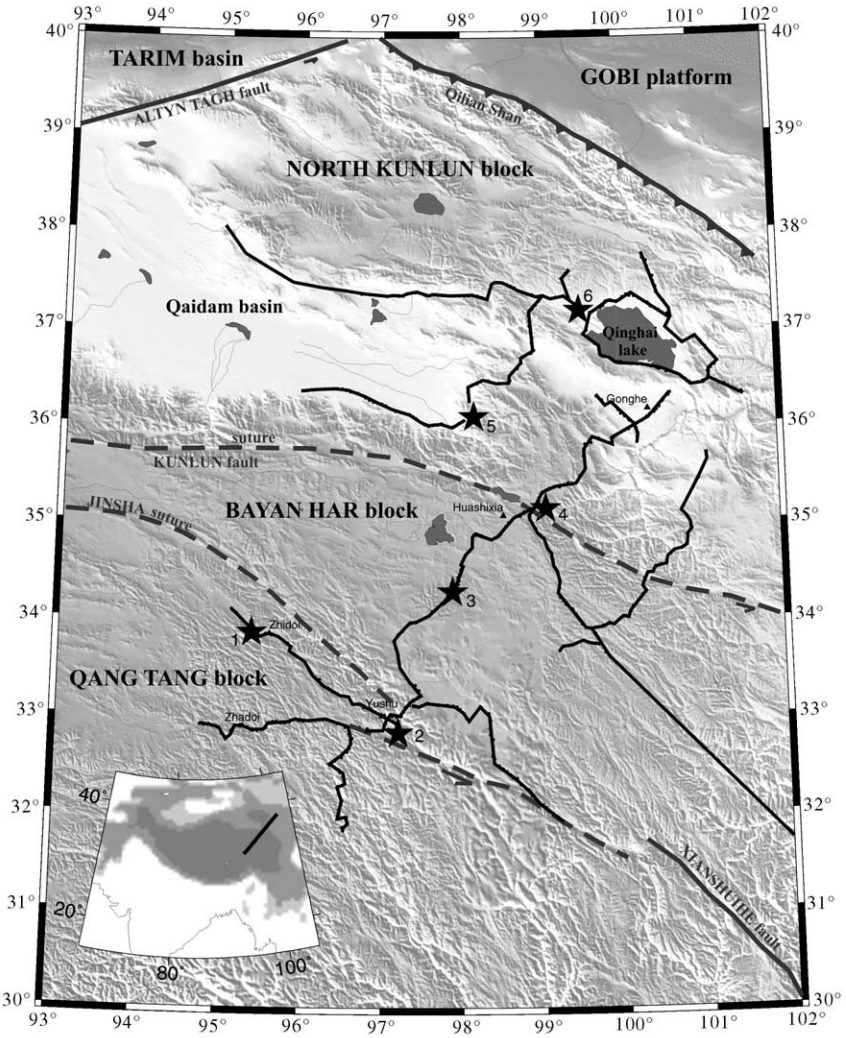

Fig. 1. Sketch map of the northeastern part of the Tibetan plateau. Black stars are shotpoints of charges of 3 to 5 ton. Black lines represent the profiles with 3-component seismometers at 5 km spacing.

attenuation was due to the crust above, and assuming twice smaller attenuation for P waves, this would yield a layer-average equivalent for the 80 km thick crust of Q_p=200. Early on also, attenuation in the lower crust of the Tethyan Himalayas could be measured from explosion seismology data and was discussed in relation to temperature and partial melt (Hirn and Sapin, 1984; Hirn et al., 1997). For the 40 km thick lower half of the crust, a significantly high attenuation or a low quality factor Q_p=125 was derived accordingly. Only the lower crust was sampled by their method, which could not have detected melt in the upper crust, such as was discussed by Pham et al. (1986) from magnetotellurics. Recently explosion seismology could be applied to Central Tibet (Meissner et al., 2004, and references therein) and Northeast Tibet. In the present survey across Northeast Tibet, Galvé et al. (2002a) inferred from amplitudes of reflected waves, that there cannot be a partial melt thickness significantly larger than 1 to 2 km in the lower half of the crust. Here we analyze constraints on Q that can be derived from these data for the lower crust at the northern edge of the Qang Tang, and at the northern edge of the Bayan Har terranes, where Jiang et al. (2005—this issue), and Galvé et al. (2002a,b) suggested lithospheric imbrication.

The set of parameters V_p, V_p/V_s, and Q deduced from wide-angle reflection and refraction profiles in Northeastern Tibet (Fig. 1, Galvé et al., 2002a; Jiang et al., 2005—this issue) and the Tethyan Himalayas (Hirn and Sapin, 1984) is used to derive implications on composition, mineralogy, temperature physical state, and evolution of the North Kun Lun–Qaidam, the northern Bayan Har, the northern Qang Tang and the Tethyan Himalayas blocks. Galvé et al. (2002a) illustrated in Northeastern Tibet, first-order contrasts between crustal blocks in the mere observed record-sections and resolved crustal architecture across the limit between the North Kun Lun and Bayan Har blocks that suggest imbrication, and documented the lack of a significant partial melt layer in the lower crust. Jiang et al. (2005—this issue) document further the structure of the Bayan Har, and the architecture across the Bayan Har to Qang Tang boundary. Here we use the parameters V_p, V_p/V_s and bracket the values of the quality factor Q in the lower half of the crust to discuss the value of temperature relative to that of the solidus.

A tentative interpretation of elastic and anelastic parameters in terms of composition, mineralogy, temperature and hydration of the lower half of the crust is thus suggested here. These features appear as contrasted at the northern edge of the Bayan Har and of the Qang Tang blocks and, together with the new elements on the architecture at the edge of these two blocks, contribute to suggest evolutionary models, with lithospheric imbrication at diverse levels that can be viewed as partial collision or subduction at different stages or which differ by their ages.

2. Lower crust V_p and V_s in the Tethyan Himalayas at the northern edge of India, at the northern edges of Qang Tang and Bayan Har: composition and metamorphic facies (mineralogy)

Discussion on crustal material composition and mineralogy has been previously limited by the lack of accurate measurements of velocities of P and even more of S-waves. These have been seldom obtained together, in particular in Tibet. Indirect inferences on crustal V_p/V_s from converted teleseismic waves are a matter of debate for North Tibet between high values (Owens and Zandt, 1997) and low values (Vergne et al., 2002). Makovsky and Klemperer (1999) recorded P converted to S upon reflection on the bright spots in the southern Lhasa block. Sapin et al. (1985) obtained full path wide-angle S waves returned from 30 km depth in the northern Lhasa block, with a clearly low V_p/V_s=1.6 that Min and Wu (1987) attributed rightly to the lowering of P velocity with increasing temperature to the alpha–beta quartz transition (Hirn et al., 1997). There, temperature deeper in the crust may reach the solidus since there is no indication of SmS propagation.

2.1. V_p and V_p/V_s: felsic composition in the North Qang Tang

In the case of the shot 2 to shot 1 strike-line in northern Qang Tang (Figs. 1 and 2a), the model with a low-velocity layer on top of the Moho of Jiang et al. (2005—this issue) did not still allow to fit well the distance of the maximum amplitude for the Moho reflection. Another characteristic not fitted is the observed low frequency of the Moho reflection with respect to the previous intracrustal one (Fig. 2a). Such low frequency of the deeper penetrating waves could be thought of as being the result of strong attenuation in the lower crust.

The PmP (T6) is clear, and its spectral content apparently contrasts with that of the previous intracrustal reflections (T5) as shown in Fig. 2b. Then, taking the simple spectral ratio technique used in the Tethyan Himalayas by Hirn and Sapin (1984), from which Q is

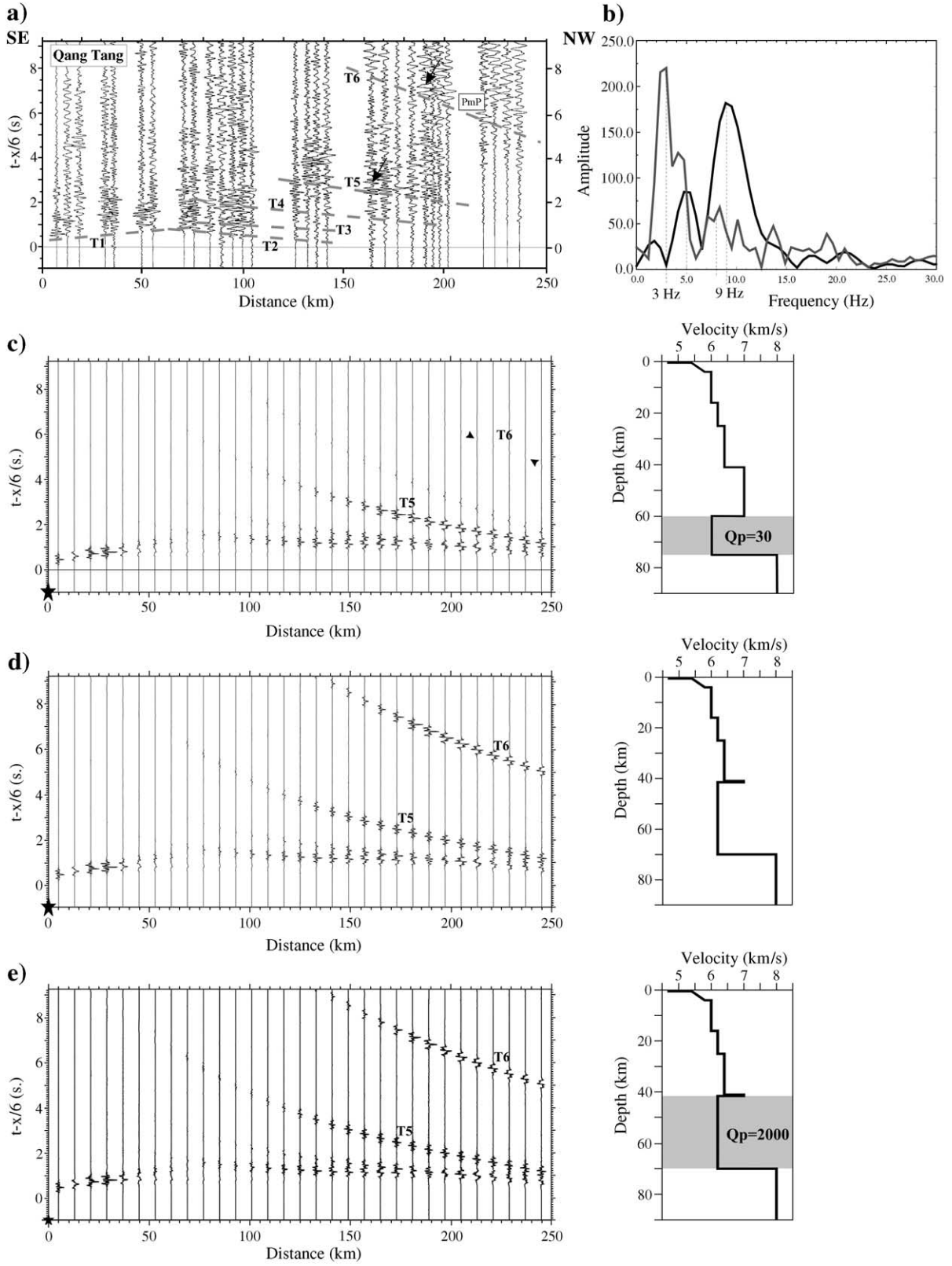
a)
SE
NW
Qang Tang
T1
T2
T3
T4
T5
T6
PmP
t-x/6 (s)
Distance (km)
b)
Amplitude
3 Hz
9 Hz
Frequency (Hz)
c)
d)
e)
t-x/6 (s.)
Velocity (km/s)
Depth (km)
Qp=30
Qp=2000

obtained from the amplitude and frequency changes observed in the waveforms of reflections above and below the layer, one may try to assess attenuation in the lower half of the crust. This yields a value for the layer-equivalent Q on the order of 70. However this value is not adequate, since at variance with the case in the Tethyan Himalayas, it is not here confirmed by full waveform synthetic seismogram modelling. This is seen in Fig. 2c, where such a value for attenuation has indeed made the PmP amplitude to disappear, and no velocity–depth model can be found to take into account such a high attenuation. Here the tentative lower crust layer-equivalent $Q_p=70$ was equivalently concentrated in its low-velocity-layer, LVL, a part in the model of Jiang et al. (2005—this issue), as a 20 km thickness with $Q_p=30$.

Because the observations evidence a high overall PmP amplitude with respect to intracrustal reflections; whereas in the Tethyan Himalayas, the PmP amplitude had to be multiplied by three to be seen with respect to the intracrustal reflections (Hirn and Sapin, 1984), attenuation in the lower half of the crust is unlikely a dominant cause for the lower frequency of PmP. This is also consistent with the fact that SmS are observed here, which would be even more affected by attenuation.

The observations suggest that high frequencies in the incident signal would here be preferentially reflected at the mid-crustal high velocity interface while the low frequency part is transmitted through it to propagate to depth and being reflected on Moho. An alternative cause for the separation in frequency between reflected and transmitted wave can indeed be provided by particular interaction with heterogeneity. This can be approached by thin-layering to give the so-called quarter wavelength effect on signals and more specifically here cause wave-tunnelling effects (Fuchs and Schulz, 1976). Then the thin layer, or scale of heterogeneities between upper and lower crust reflects the higher frequency part of the signal, whereas it allows the lower frequency part to be transmitted across it, propagate through the lower crust and be reflected to the surface as the PmP, in a proportion that varies with the angle of incidence. In Fig. 2d, a high velocity thin layer is introduced in the model at mid-crustal depth to represent the effect of such change in scale length of heterogeneity. Velocity beneath can then be taken as small as the 6.2–6.4 km/s value which is necessary above the Moho in order to achieve the high-amplitude at short distance for PmP with such a large crustal thickness. Together with a moderate value of 1.73 for the average crustal V_p/V_s velocity ratio (Jiang et al., 2005—this issue), this establishes its felsic nature.

2.2. A felsic lower crust sampled from the Tethyan Himalayas to the North Kun Lun–Qaidam blocks

According to Galvé et al. (2002a), the presence of S-wave Moho reflections, SmS, allowed to constrain in the North Kun Lun–Qaidam block an average $V_p/V_s=1.73\pm0.01$. Jiang et al. (2005—this issue) found in the north Qang Tang that the strike-line rather unexpectedly documents shear wave propagation down to Moho with SmS that, although lacking sharp onsets above noise define by comparison to PmP, the average crustal V_p/V_s to be also as low as 1.73 ± 0.02. In the north Bayan Har, a very low V_p/V_s is measured, smaller than 1.6 for the lower crust. They show that even if there was anisotropy in the lower crust (Sherrington et al., 2004) the material would have a V_p/V_s still below 1.73. Assuming a felsic upper crust for the North Kun Lun–Qaidam and the Qang Tang blocks as observed by Vergne et al. (2002) with a velocity ratio of 1.73, the average value of 1.73 found in these blocks implies a similar V_p/V_s of 1.73 for the lower crust.

Then the velocity ratios in the lower crust of these blocks appear equal or lower than 1.73, that is signif-

Fig. 2. Modelling of Shot 2 towards WNW on the strike-line in northern Qang Tang.

a) Observed record-section with a velocity reduction of 6 km/s, showing a strong Moho reflection T6 with strong amplitudes at short distance and lower dominant frequency signal than in earlier reflections T5, as indicated by arrows on records.
b) Spectra of the PmP (gray line) and of the intracrustal reflection (black line) on records pointed by arrows in a) respectively at 190 and 160 km.
c) Synthetic record-section for a model containing a low velocity layer on top of the crust–mantle interface as in Fig. 5 of Jiang et al. (2005—this issue). A $Q_p=30$ is introduced in the LVL in order to account for the observed spectral ratio of the PmP and intracrustal reflection if it were due to attenuation. PmP (arrows) cannot be distinguished at variation with observations. The velocity model brings to short offsets the critical distance for Moho reflection T6 but does not model its contrast in dominant frequency with earlier reflections.
d) Synthetic record-section for a model with a mid-crustal high-velocity thin-layer lid to the low velocity layer on top of the crust–mantle interface of the previous model This allows to fit by the tunnelling effect of the thin-layer lid, the lower dominant frequency of this wave transmitted through the mid-crustal thin-layer lid with respect to the higher dominant frequency of the wave T5 reflected from this lid, as observed.
e) Synthetic seismograms for the same velocity model but where a Q_p of 2000 has been introduced in the low velocity layer, corresponding to the maximum attenuation we can introduce, keeping the observed PmP amplitudes.

icantly lower than the average for a continental crust which is 1.77 to 1.78 according to Christensen and Mooney (1995) and Zandt and Ammon (1995). In addition to this low velocity ratios, Jiang et al. constrain a P-wave velocity in the lower crust of the Bayan Har of 6.8–7.0 km/s while we found a velocity of 6.2–6.4 km/s for the lower crust in the Qang Tang. Together with the low V_p/V_s ratio, these Vp values are so low that the data for the lower crust of the Qang Tang and the Bayan Har plot in the felsic field of the measurements of Christensen (1996).

In addition, we can consider the results obtained in the Tethyan Himalayas block by Hirn and Sapin (1984). They derived a V_p=6.4–6.6 km/s and considered the material as dominantly felsic, since no other composition could give so low values at such high pressure.

In their study of elastic parameters in anhydrous rocks from monomineralic parameters, Sobolev and Babeyko (1994) model the density and both P- and S-wave velocities for different compositions, at equilibrium in different mineralogical states that are a function of pressure and temperature, as well as their corresponding pressure–temperature derivatives of the velocities to account for their corresponding in situ conditions.

Accordingly, the low values of V_p/V_s in addition to the V_p values observed here establish that the material forming the sampled lower half of the present crust in these blocks is felsic and can only be granitic to slightly granodioritic.

2.3. Lower crust V_p and V_p/V_s: composition and equilibrium mineralogy: in situ temperature

Knowing now that the composition is granitic from granodioritic and knowing the P-wave velocity of the lower crust, we can attempt using the calculated pressure–temperature diagram with velocity isolines from Sobolev and Babeyko (1994) to deduce the lower crust geotherm in the northern part of the Qang Tang and of the Bayan Har blocks, as well as in the Tethyan Himalayas.

As two extremes plausible compositions, a pure granite, and a granodiorite intermediate between granite and diorite are illustrated in Fig. 3 by their constant-V_p isoline curves with in situ values of 6.2, 6.5, and 6.9 km/s in the pressure–temperature field, according to the velocities given by Sobolev and Babeyko (1994) or derived from their relations. In the northern Qang Tang, the waveform modelling taking into ac-

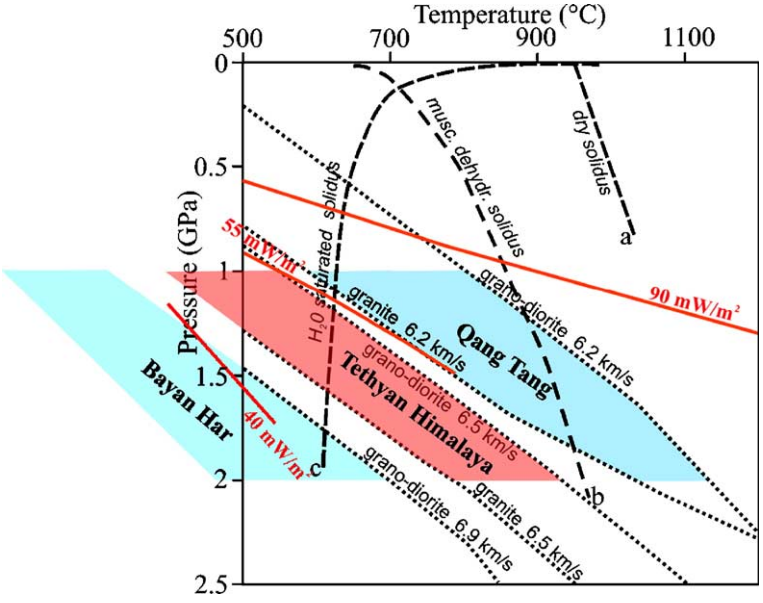

Fig. 3. Pressure–temperature field, solidus curves, conductive geotherms and velocities in lower crust of different blocks in Tibet.

– Dotted lines are in situ constant velocity lines, iso-V_p lines. Noted granite 6.2 and 6.5 km/s according to the phase diagram, and noted granodiorite 6.2, 6.5 and 6.9 km/s for intermediate composition interpolated between the granite and diorite diagrams of Sobolev and Babeyko (1994).
– For the different regions discussed, the relevant lower crustal velocity fields are identified by their names in the P/T diagram. Qang Tang with V_p=6.2 km/s; Tethyan Himalayas, south of Indus–Tsangpo suture with V_p=6.5 km/s, Bayan Har with V_p=6.9 km/s.
– Conductive geotherms for standard, low, average and high heat flow values are sketched in red (after Christensen and Mooney, 1995).
– Dashed lines are granite solidus curves according to Hacker et al. (2000) for (a) dry melting, (b)dehydration melting, and (c) wet melting.

count the tunnelling effect to explain amplitudes resulted in a notably low value of V_p=6.2 to 6.4 km/s in the lower half of the crust. In northern Bayan Har, velocity may be 6.8 to 7 km/s, according to the two possible models.

When these values for Qang Tang and Bayan Har are plotted into the V_p grid in the *P–T* field of Fig. 3 and taking into account the uncertainties we have on the P-wave velocities, a number of major features emerges:

- There is no overlap among the temperature ranges for the two blocks, whichever different compositions in the range granite–granodiorite correspond to the each of them.
- Temperatures are significantly lower in the Bayan Har than Qang Tang lower crusts.
- Temperatures among the two regions differ at minimum on the order of 290 °C, if compositions were the same.
- For Bayan Har, temperature is below 670° at 75 km depth, for any different composition in the plausible range, even in the extreme granodiorite compositions.
- For Qang Tang, temperatures may be as high as 1100 °C at 75 km and 800 °C at 40 km depth, if the extreme, granodiorite composition is assumed.
- In Qang Tang, the velocity isolines from the present seismic observations plot remarkably into the limits of the geotherms determined for the Qang Tang xenoliths by Hacker et al. (2000) using the V_p depth variations derived from wide-angle reflection modelling of INDEPTH III.

In addition we may plot here the results obtained by Hirn and Sapin (1984) in the Tethyan Himalayas, south of the ITS, where they derived for the lower half of the crust a V_p of 6.4 to 6.6 km/s.

The temperatures in the lower crust of the Tethyan Himalayas appear then being higher than in the ones in the Bayan Har block and they overlap the ones of the Qang Tang block. The maximum temperatures in the Tethyan Himalayas appear to be of 640 °C at 40 km depth and of 985 °C at 75 km depth.

3. Estimation of *Q* values in the lower half of the crust

3.1. Explosion seismology and attenuation

Amplitude of a seismic wave decreases upon propagation as $\exp(-\pi FLV_p^{-1}Q_p^{-1})$ i.e. as an exponential with the inverse of the quality factor Q_p, the frequency F, the length of the ray path L, and the inverse of the velocity value V_p. These parameters have very specific values in wide-angle reflection explosion seismology, with signals centred in the 2 to 10 Hz frequency range and long, two-way, oblique paths on the order of a hundred kilometres in the crustal layers. Its signal spectrum and propagation path provide favorable conditions of sensitivity of amplitudes to attenuation of moderate magnitude. Using a differential approach by comparing waves reflected on top and at the base of the lower crust, they allow to ignore the unknown source amplitude spectrum and the propagation through the upper crust since they are the same for the two waves. However they are also sensitive to the effect of the velocity depth function on amplitudes that must be taken into account. Then the difference in path lengths between the mid-crustal reflections and the Moho reflections is on the order of four times the thickness of the layer in between the two reflectors because of the two-way path and oblique incidence. This allows the effect of a wide range of significant attenuation values in the lower crustal layer between those reflectors to be evidenced by comparing the relative amplitude levels as well as the waveform of the two reflections.

For the two frequencies of 3 and 8 Hz, that are in the bandwidth of the wide-angle reflection signals recorded in Tibet from the top of the lower crust and the Moho, a quality factor from a few tens to thousands gives effects that can be seen in the waves and thus can be measured. For a significant but not extreme attenuation with a Q of 500 over a 25 km thick lower crust reduces amplitudes at 3 Hz by a measurable 23% and at 8 Hz by a strong 57%. A similar reduction is obtained if Q=50 in a 5 km thickness layer.

For teleseismic body waves that have a frequency of an order of magnitude lower as well as a shorter, steep one-way crustal path, a Q value as low as 50 in a 25 km thick lower half of the crust decreases the amplitude of 2 s period teleseismic signals by only 12%. Hence even such a strong attenuation, that corresponds to the presence of partial melt in the lower crust, is hardly detectable. With the higher frequencies of vertical reflection seismic, attenuation cannot be measured when significant, since it is the signal itself that cannot be seen anymore. Indeed the same Q_p=50 in the lower crust reduces the amplitude at 20 Hz by 99%, and still by 88% for only a 5 km thick layer with this attenuation.

Thus, among seismic methods, wide-angle reflection seismic has a unique sensitivity to Q values in the range of 10 to 1000 in crustal layers of 1 to 50 km

thickness, due to the source frequency-band and the path geometry. On the other hand, to use reflected waves for attenuation measurements, the dependance of amplitude on frequency of the reflectivity as a function of the type of localized velocity contrasts at the turning points of the reflection has to be evaluated. Also the frequency-dependent loss of amplitude in transmission for the deeper penetrating wave with respect to the shallower one has to be checked, as has been illustrated on the case of North Qang Tang discussed in Section 2.1.

3.2. Bayan Har lower crust layer-average Q estimates

For the *Bayan Har* we may derive a lower bound to the value of average Q_p in the lower half of the crust from the variation of the amplitude–frequency level of reflections turned back from the Moho at 70 km as compared to the reflections on the middle crust interface at 35 km (Fig. 4b), as done by Hirn and Sapin (1984) for southern Tibet. For this, we model the two waves with full-waveform synthetic seismograms including the effect of attenuation (Fuchs and Mueller, 1971; Kennett, 1975). In applying this relative method to estimate Q in the lower half of the crust, the source amplitude spectrum, and the heterogeneity or attenuation in the upper half do not need to be known, and also cannot be obtained. We only constrain Q in the lower half of the crust. In practice we use an elastic model from the surface to the interface giving the intracrustal reflection and a source spectrum giving the signal observed for this reflection. Then, we model this reflection and the next one at the Moho by searching a range of velocity–depth models to find the lower bound of values of path-averaged Q_p in the lower half of the crust that give still the observed Moho reflection amplitudes.

The 2D model obtained by Jiang et al. (2005—this issue) in this block shows that there is no strong lateral change of velocity or structure over the offsets we are looking at. However, we have to assume in this study that the site effects have the same consequences on amplitude at all stations.

An upper bound on attenuation, lower bound on Q, with $1000 < Q_p$, is thus constrained, since for higher attenuation, no model is found with a velocity contrast as high as reasonable that would give a Moho reflection strong enough with respect to observed amplitudes, and satisfying travel times. This is shown in the synthetic seismograms of Fig. 4. There, the Moho has the highest possible velocity contrast among the types of models considered by Jiang et al. (2005—this issue), with a low-velocity-layer lower crust, which response with no attenuation is shown in Fig. 4c. In Fig. 4d, with $Q_p = 1000$ in the lower crust, the relative amplitude of the PmP with respect to the reflection at 30 km depth is smaller and has lost its high-frequency part but may be considered still of an acceptable magnitude, hence give an upper bound to attenuation. PmP amplitude decrease significantly with $Q_p = 500$ (Fig. 4e) and has become indistinct with $Q_p = 250$, as shown in Fig. 4f with respect to Fig. 4c.

On the other hand, if we assume that the absence of SmS in the Bayan Har is only due to attenuation, an upper bound on Q can in turn be estimated from the S-wave record-section. Indeed in contrary to the P section, we do not observe S-wave reflections on interfaces deeper than the strong intracrustal one, not even on the Moho. Since S waves spends 1.7 times longer than P waves in the medium, then in the model response of Fig. 4 with times and reduction velocities scaled by V_p/V_s, the amplitudes shown can be equally taken as those of S waves for Q_s values 1.7 times the value of Q indicated. That is, model amplitudes get indistinct as observed for Fig. 4e, that is $Q_s < 850$. Since $Q_p \sim 2Q_s$ (Kampfmann and Berckhemer, 1985), if this evidence from absence of SmS waves is transformed to Q_p values, it gives an upper bound value for $Q_p < 1700$, that is a lower bound on attenuation.

The only instance of SmS recording from a shot in the Bayan Har is from Shot 3 on the line of stations that was located to reach into the North Kun Lun–Qaidam

Fig. 4. Constraints on Q provided by the observations on the lower crust of the Bayan Har. (Shot 4 to SW)

a, b) Observed record-sections in the Bayan Har blocks, with a velocity reduction of 6 km/s, respectively, of Shot 4 to the southeast and of Shot 4 to the southwest.

c) Synthetic seismograms for a crustal model of the Bayan Har with a high velocity mid-crustal reflector and a lower velocity lower crust beneath, one of the two types of models considered by Jiang et al. (2005—this issue), the other one is displayed in their Fig. 4c and features an intracrustal low velocity layer at around 30 km depth.

d) Synthetic seismograms of the largest offset records for the same velocity model but where a Q_p of 1000 has been introduced in the 35 km thick lower crust.

e) Same as d) but with a Q_p of 500, which significantly reduces the PmP amplitude to practically undetectable.

f) Same with a Q_p of 250.

block in order to sample the Moho under the Kun Lun fault (Fig. 2). Up to half the ray path is then in the North Kun Lun block, in which attenuation did not appear significant, since SmS that have their whole path in the North Kun Lun are well observed. Hence with only half their path in Bayan Har, SmS are seen, whereas with a

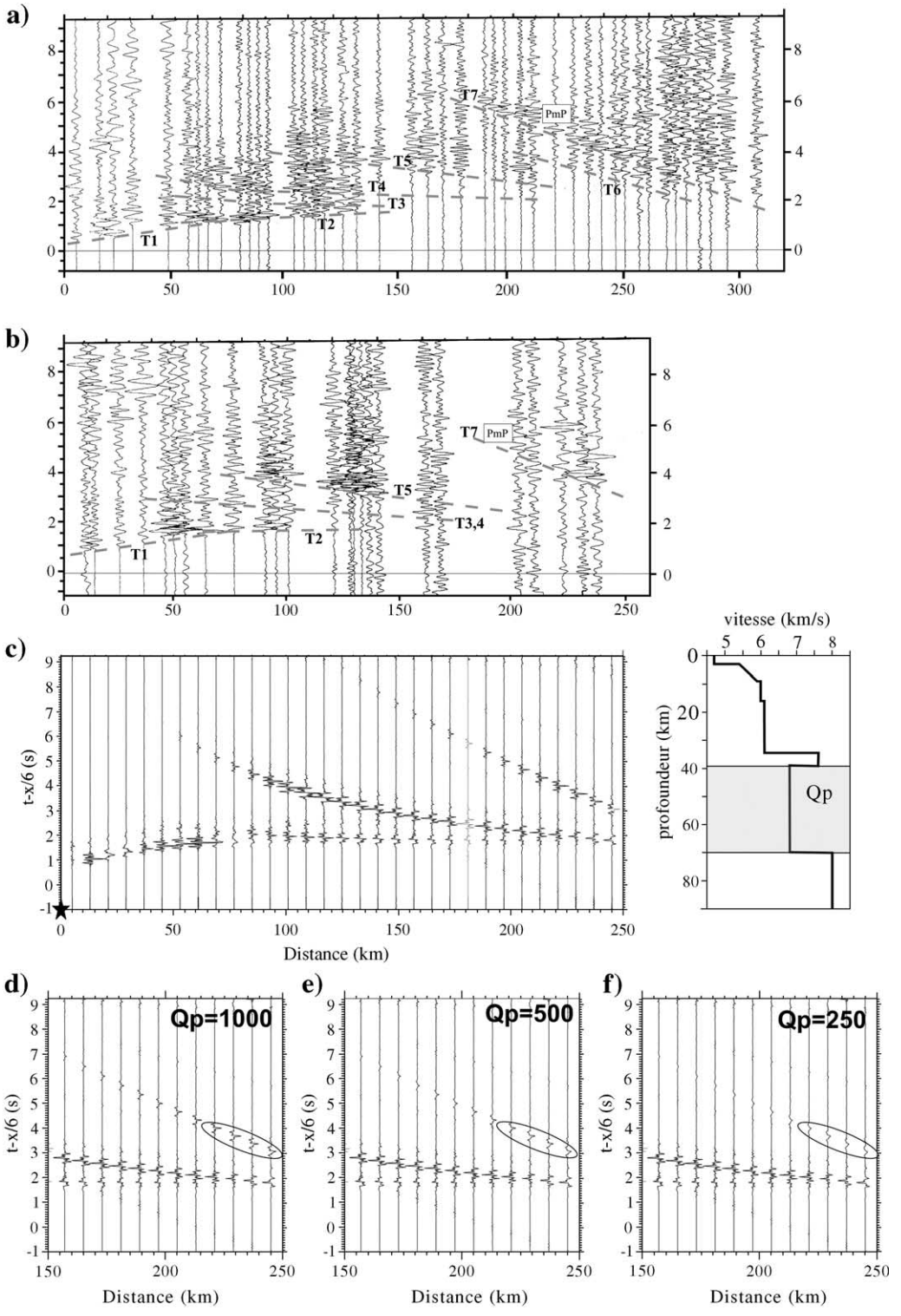

full length path they were not. This has several implications. That in this case SmS is seen here for a shot and reflection points in the Bayan Har, as PmP was, establishes that when SmS is not seen this is not due to a difference of the Bayan Har Moho reflectivity in the P and S modes. Hence it was justified above to derive a lower bound on attenuation, in this case $Q_p<1700$, from the absence of SmS for full path length in Bayan Har. It is the effect of attenuation that affects S amplitude more than P, the longer its path in the lower crust of the Bayan Har. We can then use the observation that with only half the propagation path in the attenuating lower crust of the Bayan Har, SmS is seen here as well as PmP was seen for a complete propagation path in the Bayan Har. This constrains the upper and lower bounds on Q to be in a factor of 2 and hence confirms the lower bound on $Q_p>1000$.

Combining the modelling of the presence of Moho reflections in P with their absence in S, while reflections from the mid-crustal interface are obtained in both modes, allows to bracket the value of the quality factor in the lower half of the crust. This is confirmed by the presence of S Moho reflections in a particular geometry where only half the path is in the Bayan Har lower crust. The layer-equivalent quality factor Q_p, average value over the whole 35 km thick lower crust of 6.8–7.0 km/s velocity is comprised between about 1000 and 2000.

3.3. North Qang Tang: lower crust layer-average Q estimates

The tunnelling effect dominates the amplitude–frequency behaviour between reflections above and below the lower crustal layer. We may still model with anelastic full waveform synthetics including both the tunnelling and attenuation effect, in order to derive constraints on the value of Q. In Fig. 2e, with $Q_p=2000$ the PmP has lost more amplitude in the high frequency domain. Its maximum amplitude is lower with respect to the intracrustal reflection and is shifted to slightly larger distance. This may be an upper bound on attenuation. But a lower value of the upper bound on attenuation is indeed provided by the fact that clear SmS are recorded. If we scale as before the image of Fig. 2e for the velocity and for the ratio of attenuation of the two waves, the presence of SmS requires a lower bound of $Q_p>7000$. This appears consistent with the fact that in the Bayan Har their absence required an upper bound of $Q_p<1700$, given the difference in velocity–depth models and contribution of tunnelling effect.

4. Q, low-velocity layers, partial melt and lithology of the lower crust through Tibet

4.1. Attenuation and low-velocity layers in the lower crust of North Central Tibet: not partial melt inclusion but buried upper crustal lithology

The crustal velocity depth-modelling of Galvé et al. (2002a) for the northern edge of Bayan Har as well as by Jiang et al. (2005—this issue), for the northern edge of Qang Tang, constrained the need of considering LVL, low-velocity layers in the crust. In the preferred models, these form the whole lower half of the crust, under a reflecting, high-velocity lid (Figs. 4c and 2d). If the LVL had its cause in the low velocity of $V_p<6.8$ km/s relative to the lid of $V_p>7.3$ km/s as being induced by the effect of increased temperature on a same crustal material, the velocity reduction implied is so large that melting would be required. According to parameters of Kampfmann and Berckhemer (1985) and Sato et al. (1989a), the rate of P-velocity decrease is more than 6% per 100 °C temperature increase above solidus, in contrast to more than twice smaller under the solidus.

In order to evaluate what such partial melt in the whole LVL would mean for attenuation, the value of the quality factor at the solidus, Q_m, has to be considered. It has been measured principally for mantle and magmatic rocks. Berckhemer et al. (1982) and Kampfmann and Berckhemer (1985) obtained for Q_p at the beginning of partial melt a value of 30 for dunites and 10 for gabbros. According to Sato and Manghnani (1985), Sato and Sacks (1989), Sato et al. (1989b) and Sato (1991), Q_p at solidus is equal to 20 for peridotites and between 2 and 15 for andesites. Jackson et al. (1992) obtained a value of Q_p of 50 just under the solidus temperature of dunites.

Galvé et al. (2002a) took from all these studies a value of $Q_p=30$ at the solidus as an upper bound for lower crustal rocks, which will be documented later. They showed then, from the high ratio of observed PmP to intracrustal reflection amplitude levels that a partial melt layer in the lower crust would have an upper bound of only 2 km in thickness under the Bayan Har and less than half this value under the Qang Tang. This very small thickness makes a partial melt layer an unlikely cause for the observed attenuation, and moreover for the low-velocity in the lower crust.

Attenuation measurements are thus in support of the interpretation of low velocity value in the lower half of the thick crust as being indicative not of partial melt but of presence of material of upper crustal

lithology. The detection of material of such upper crustal lithology at these large depths then implies that large scale thrust or subduction tectonics has led it to be transported down.

4.2. Lower crustal Q and melt through Southern and Northeast Central Tibet

We now have estimated values of the lower crustal quality factor Q_p at different places across the Tibetan Plateau, from the present survey and other ones having similar resolution in the southern half of Tibet.

Indeed, between the Himalaya and the Indus–Tsangpo suture, ITS, explosion seismology provided Moho wide-angle reflections that appeared very clear along a strike line (Hirn et al., 1984; Hirn and Sapin, 1984). However these clear Moho reflections had an amplitude level only one third of that of the mid-crustal reflections at shorter offset and had to be magnified accordingly by a factor of three for display in Fig. 2 of Hirn and Sapin (1984). Then, they appear as clear and strong over the background noise, which is because of the great strength of the shots, 10 or 20 tons of explosives in water. A lower crustal layer-average Q_p of 125 was obtained.

In the present survey through whole Northeast–Central Tibet, the wide-angle Moho reflections appear weak with respect to the background noise level. But the same is true for all other waves and this is because of the shots that were weaker by about an order of magnitude than in the southern Tibet, with their charge size being 1/4 and shot in drillholes instead of lakes. At variance with the case of the southern Tibet recalled above, Moho reflections and the shallower reflections have here similar amplitude levels. In addition SmS, S-wave Moho reflections are clearly recorded on several profiles in northern Qang Tang, northern Bayan Har, and North Kun Lun–Qaidam, whereas none could be found in whole Tethyan Himalayas. These clear and simple responses of the medium to the explosion seismology design establish a first order feature of the lower crust: in northeast–Central Tibet, attenuation is less, that is Q_p is higher, than in the Tethyan Himalayas, south of the Indus–Tsangpo suture.

South of the ITS, if the lower crust average $Q_p = 125$ would be due to partial melt localized in a layer, this would have to be four times thicker than in Bayan Har, with a thickness on the order of 4–8 km that begins being significant. Far north of the ITS, on the northern edge of the Lhasa block, only low amplitude PmP could be obtained (Sapin et al., 1985). This weakness, if not due to structural complexity of the interface as the profile was recorded close to the Banggong Nujiang suture, would suggest a more important partial melt portion in the crust in the Northern Lhasa block than south of ITS.

A spatial variation is indeed evidenced from the Himalayas through the Lhasa block and into Qang Tang, when teleseismic waves are considered, which sample the whole crust and upper mantle. The relative S residuals increase out of normal proportion to P when going northwards, which can be interpreted as an increase from the Himalayas into Qang Tang of the cumulative amount of melt taken through the whole crust and topmost mantle (Hirn et al., 1995, 1997; Sapin and Hirn, 1997). A crustal part to this northward increase in partial melt fraction can be documented from the increase across the ITS in its crustal average V_p/V_s established by the joint wide-angle reflection and receiver-function observations of Galvé et al. (2002b).

In contrary, further North, as shown here in North Central Tibet from northern Qang Tang through Bayan Har, no significant melt is present in the lower half of the crust. Magnetotelluric measurements on a transect across whole Tibet are indeed in accordance with such a view. A high-conductance anomaly had been evidenced in southern Tibet and attributed to temperature effects with fluids and partial melt by Pham et al. (1986). Wei et al. (2001) find on their transect of whole Tibet an increase in total conductance of the lithosphere from south Tibet into Qang Tang. However, northward of mid Qang Tang, they establish a strong decrease in conductance, hence decrease in partial melt fraction.

5. Q-derived homologous temperature, with composition and temperature from V_p and V_s. Particular solidus: wet, dehydration, dry melting material conditions

5.1. Q and homologous temperature (ratio of in situ to melting absolute temperatures)

In contrast to V_p, V_s, and V_p/V_s that see the melting point, Q instead has a variation with temperature that is the same above and below the solidus, but which is exponential. More specifically, Meissner and Vetter (1970) suggested that the logarithm of seismic Q followed a linear relation with the inverse homologous temperature, the ratio of solidus to in situ absolute temperatures.

Indeed, Kampfmann and Berckhemer (1985) measured Q as a function of temperature and frequency at constant pressure for different rock types and similarly

concluded that the attenuation factor followed a power-law dependance of the form $Q^{-1} \propto \exp(-A'/RT)$, with absolute temperature T, for $T > 0.8\ T_m$, T_m being the solidus absolute temperature, and R is the gas constant. A', an apparent activation energy depends on the nature and composition of the rock, with the lowest value corresponding to silicic or wet samples that have also the lowest solidus temperatures. Hence Q normalized to its value at melting (Q/Q_m), it appears merely a function of the homologous temperature T/T_m (K), since this takes into account the particular rock composition and state. As for the dependance on pressure, it is similarly included in the normalization to melting temperature. This has been shown by Sato et al. (1989a) and Sato (1991) who measured different values of attenuation for a same material at different pressures and could relate their variation with the pressure dependance of its solidus temperature.

Since the lower half of the crust definitely appears as of felsic lithology and we sample it in a specific frequency band, we may check that these conditions do not lead to Q_m far from the general case of more abundant measurements mentioned in Section 3, as implied in the discussion of significant absence of lower crustal melt by Galvé et al. (2002a). Among the rocks considered by Kampfmann and Berckhemer (1985), the most acidic and silicic igneous rock, a phonolite vulcanite has the lowest solidus of about 920 °C, a value close to that of granite. Their results at 5 Hz, in the band of the present explosion seismology experiment, show a threshold of significant attenuation with $Q = 1000$ being reached at 620 °C. This is a homologous absolute temperature of $900/1200 = 0.75 T_m$. Measured Q decreases to a Q_m between 20 and 50 at T_m. This is in keeping with the general relation of Sato (1991) for diverse pressures and rocks obtained between 0.85 and 1.06 T_m when it is extrapolated to $T = 0.75$ Tm resulting consistently in $Q = 35 Q_m$.

With this relation, Q on the order of 125 for Tethyan Himalayas implies homologous temperature $T/T_m = 0.87$. Values of the quality factor of $1000 < Q_p < 2000$ for Bayan Har imply homologous temperature between 0.74 and 0.77. The Q value for northern Qang Tang is too high that the relation of Sato (1991) can be used to derive a value of homologous temperature, which is significantly below the other cases. Then even if the lower crusts of Bayan Har and Tethyan Himalayas are not in the thermal regime of partial melt, the homologous temperatures are quite high and the ductile limit commonly considered to be at a homologous temperature on the order of 0.7 may be reached.

5.2. Homologous temperature and in situ temperatures: relevant solidus and hydration conditions

This homologous temperature we obtained for the lower crust in the north Bayan Har, the north Qang Tang and the Tethyan Himalayas can be considered together with the geotherms we previously obtained from V_p and V_p/V_s (Fig. 3), in order to estimate the in situ material properties with respect to wet, dehydration or dry melting conditions.

Under the northern edge of the Qang Tang, a low attenuation is sampled in the lower crust, with a Q value of several thousands. When estimated from the velocity value in the phase diagram of Fig. 3, the corresponding temperature is higher than the wet solidus. Since there is no melt, this temperature indicates that the dry or the dehydration-controlled solidus applies for the material. In addition, we constrain a homologous temperature that has to be lower than 0.74, hence the dry solidus applies. This suggests that only dry conditions should prevail at present in this lower crustal domain.

In the Tethyan Himalayas, south of the Indus–Tsangpo suture, V_p/V_s is not available because of lack of detectable SmS. The 6.4 to 6.6 km/s value for V_p in the lower half of the crust below 35 km depth derived by Hirn and Sapin (1984) is considered as indicating felsic composition, since in the Sobolev and Babeyko (1994) results there is no other rock in equilibrium phase at this pressure with such an in situ velocity, but the felsic granulite (Sapin and Hirn, 1997). Such lower crustal V_p value is between those of the Bayan Har and those of the Qang Tang (Fig. 3). But attenuation is highest, and significant with a layer average Q of 125 indicating high homologous temperature, consistently with the lack of observation of S-waves. With respect to Qang Tang, the in situ temperatures are lower but since attenuation is higher, homologous temperature is higher, hence the relevant solidus cannot correspond here to the dry solidus conditions. In the case of the Tethyan Himalayas, the P–T field defined by V_p is indeed crossed by the wet-solidus. Interpretation is then less straightforward than for the first-order result noted above.

Under the northern edge of the Bayan Har the same granite–granodiorite grid applies because V_p/V_s is low. Compared to Qang Tang, the V_p is higher on the order of 6.8–7.0 km/s, indicating lower temperature. However, attenuation is higher, Q being of 1000–2000. This indicates higher values, of 0.74–0.77, for the homologous temperature, and consequently a lower temperature for the relevant solidus. This higher atten-

uation for a lower temperature indicates that the relevant material is in a more hydrated state for a similar felsic composition.

What seismic observations basically constrain are values for lower crust layer-average V or Q, but these may not be layer-constant values. Their possible variations through the layer need to be considered since, although none is well resolved, they have different implications on temperature.

For V_p, the seismic observations do not require a significant velocity gradient through the lower crust. A constant velocity could however be accounted for by different models. One is in an isothermal lower crust, where velocity could remain constant with depth if the composition changed from the granodioritic case on top to the granite case at the bottom, which would imply and inverted compositional layering. More likely, the constant V_p indicates that the lower crust has a rather constant composition. For such a constant composition, constant V_p lines are plotted in the P/T diagram of Fig. 3. Their slopes imply a significant increase in temperature with depth, but which is close to that of a normal conductive geotherm. When plotted in Fig. 3, a cold geotherm, corresponding to low value of surface heat flow such as of 40 mW/m^2, and an average geotherm for a heat flow value of 55–60 mW/m^2 such as for the Eastern US (Christensen and Mooney, 1995) straddle the upper edge of the P–T field corresponding to Vp for Bayan Har and Tethyan Himalayas. A slight change in composition from granite to granodiorite with depth would have the velocity to increase less steeply with depth than the isovelocity lines for constant compositions, implying an even stronger change of the temperature with depth.

Within the P–T field defined by the observed V_p, solidi have a slope very different from the isovelocity lines, with temperature increasing less with depth, or even decreasing as for the wet-solidus. The layer-average Q retrieved from data does not resolve variation with depth through the lower crust, but Q should relate to homologous temperature. Since even if there is no gradient in V_p, temperature increases with depth, it is not straightforward that V_p and Q be both constant through the layer. There are two end-member cases. If we take Q as constant, then homologous temperature is constant too, and the relevant solidus can then not be the same at the top and the bottom of the lower crustal layer, since the in situ temperature changes. Alternatively, if hydration conditions, hence relevant solidi are the same throughout the layer, then Q changes through the layer with respect to the average.

In this perspective, in the case of Tethyan Himalayas the wet-solidus cannot control the whole layer thickness since it crosses the V_p field. The wet solidus applies to the top of the lower crust, while the deeper part is in dehydration–melting solidus conditions. Another possibility is that the dehydration solidus applies to the whole layer, in which attenuation would increase then with depth. The situation is similar for the Bayan Har with more reduced values for the homologous as well as in situ temperatures.

6. Discussion

Composition, temperature and metamorphic facies of the lower part of the thickened crust, have been discussed before with respect to the petrogenic models of Sobolev and Babeyko (1994) from lithospheric layer velocities and thicknesses for Tethyan Himalayas by Sapin and Hirn (1997) and for central Tibet by Hirn et al. (1997). The new observations in North–Central Tibet can also be reviewed together with those, in regard of geodynamical modelling of Henry et al. (1997) and Le Pichon et al. (1997) considering only the movement of convergence between blocks.

According to Sobolev and Babeyko (1994), with increasing pressure the general trend is for V_p to increase and for V_p/V_s to decrease, due to high pressure phase transitions from plagioclase-bearing to garnet and clinopyroxene-bearing rocks. The phase transitions that correspond to the largest V_p step towards the eclogite value occur indeed at lower pressure the more basic the material composition is. This is schematized by the different plagioclase-out, Pl-out, curves that are indexed G for granite, D for diorite and B for basic in Fig. 5. These can be taken as the corresponding high-temperature granulite to eclogite transitions. The left-hand edge of Fig. 5 at 500 °C is then approximately the isothermal limit of the eclogite facies from the lower temperature facies: blueschist at high pressure and greenschist at lower pressure.

South of the Indus–Tsangpo suture, Sapin and Hirn (1997) suggested that their measurement of a low V_p=6.5 km/s in the lower crust may correspond to felsic high-temperature granulite facies. They suggest that if a basic layer may have existed in the original crust, it would now be eclogitized and located under the present seismic Moho, the transition zone at Moho being possibly due to the material of intermediate composition, leaving the crustal medium above dominantly felsic, a mechanism also considered by Beck and Zandt (2002) for the Andes.

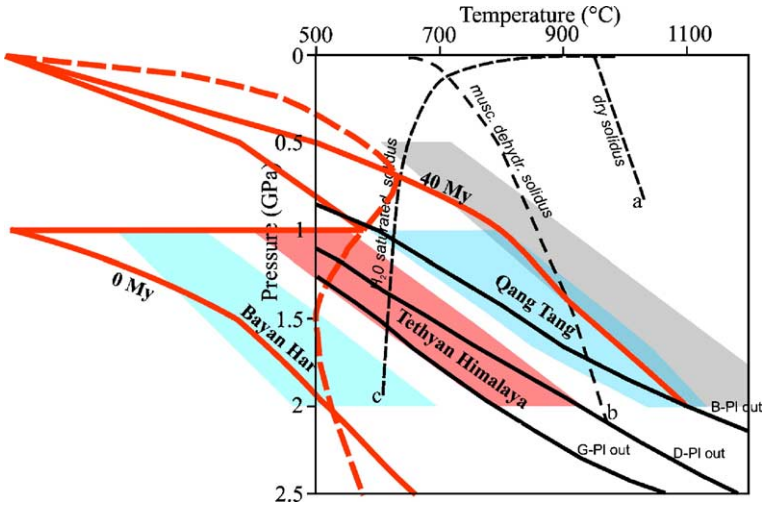

Fig. 5. Pressure–temperature field, metamorphic transitions, solidus curves and non-conductive geotherms in lower crust of different blocks in Tibet

– Coloured fields identified by region names correspond to their V_p value as in Fig. 4 and dashed lines are the similar solidus curves.
– Black lines represent the transition from high-temperature granulite to eclogite facies schematized by their Plagioclase-out curves, for granitic, dioritic and basic compositions labelled respectively by their initials.
– In gray is the field of the geotherm of the Qang Tang lower crust derived from xenolith (Hacker et al., 2000).
– In red, non-conductive geotherms as indicated:
0 My is a "subduction geotherm", obtained by instantaneous superposition of a continental crust on a lithosphere.
40 My is the geotherm for such a time after instantaneous superposition of two such segments of crust in the case of a constant heat flow provided to the mantle at their bottom, after Le Pichon et al. (1997).
– Dashed line is the geotherm of steady-state subduction, at 50 km from boundary, for a 20 mm/yr convergence rate and a moderate heat production of the subducting crust, after Henry et al. (1997).

Sapin and Hirn (1997) interpretation is consistent with the Tethyan Himalayas geotherm of Fig. 5, where its lower crustal temperature field determined by its V_p is consistently on the higher temperature granulite side of the felsic eclogite limit indicated by the G-Pl-out line. Instead, for basic composition, the whole depth range of the thickened crust is already on the eclogite side of the limit B-Pl-out.

In the northern Qang Tang, the relevant solidus for the lower crustal material is the dry solidus. Hence, the lower half of the crust formed of upper crustal lithology would have been buried here long enough that it is now dry and hot. Indeed the upper limit of the V_p field corresponds to a geotherm obtained by Le Pichon et al. (1997) for the temperature after 40 Myr for the case among those they considered of crustal doubling with a constant high mantle heat flow maintained at the base of the crust, by convection in the mantle. The lower crust of Qang Tang, is farther from the transition to eclogite in the felsic high-temperature granulite field than the Tethyan Himalayas (Fig. 5). However, for a basic composition, this transition to eclogite may be encompassed in the field, hence it would be possible too that a basic layer that would have been beneath the felsic thickened crust would be eclogitized. Therefore the absence of a mafic lower crust in the Qang Tang may just happen by the seismic Moho migrating up on top of an eclogitizing lower crustal material and not everywhere by mechanical delamination.

In northern Bayan Har, V_p/V_s indicates felsic composition but V_p is as high as 6.9 km/s. The discussion has to take into account that it is the one among the examples with highest V_p for a felsic composition, as well as with a Q-value which then indicates that it is far from the anhydrous conditions of a dry-solidus, and hence it only fits marginally into the velocity and phase diagram of Sobolev and Babeyko (1994). Its V_p field lies under even the coldest of conductive geotherms of Fig. 3, which hence suggests that its thickened crustal material is not temperature-equilibrated. With respect to geotherms in Fig. 5, it may be regarded as grossly located between the instantaneous whole crustal superposition (Le Pichon et al., 1997), subduction geotherm marked 0 My (Henry et al., 1997), and the type of geotherm of ongoing subduction, with adjustable parameters that is outlined in red dashed line (Le Pichon et al., 1997). Such whole crust superposition is however not exactly the condition in northern Bayan Har, since the evidence of the present architecture would be rather

for the superposition of a former thinner Bayan Har crust on deeper units of the North Kun Lun–Qaidam crust to the North. Indeed, a model of evolution is suggested in which its northern edge overrides the rocks of upper to middle crustal lithology of North Kun Lun–Qaidam that have thus been carried to high pressure while keeping the moderate temperature and hydrated conditions of a previous shallower situation and have not yet been affected by dehydration or the corresponding products have not been removed yet or caused melting. However, here also intermediate or basic material that would have been in place under the felsic part now brought to over 60 km depth may be located under the present seismic Moho, since geotherms among those cited which could be relevant may enter the eclogite field on its isothermal side from the lower temperature blueschist facies.

In the northern Qang Tang the high temperature inferred suggests a different stage or different history. Burial of material of upper to middle crustal lithology to the present deep lower crust could have occurred earlier and evolution brought to high temperature material that was anhydrous, or from which melt and volatiles were extracted. However the architecture of the present crust, may suggest a variant of the process of crustal thickening. Indeed the north dipping Moho from Qang Tang could suggest that its crust is indented by the Bayan Har. Then Qang Tang lower crust, which still has to be of previous upper–middle crustal lithology, could have been brought deeper from an already deep location, where it could have been at a relatively higher temperature and anhydrous state before this last episode. Consistently with the in situ seismic measurements provided here for the elastic and anelastic parameter, Hacker et al. (2000) report that xenoliths in Qang Tang recorded temperatures of 800–1000 °C at 50 km depth and that they indicate lower crust of northern Qang Tang not to be gabbroic, but felsic, even of metasedimentary origin, in keeping with the inference from specific elements of surface geology that upper crustal lithologies are widespread beneath central and northern Tibet (Kapp et al., 2003).

7. Conclusion

Velocity values derived from wide-angle reflection refraction experiments in Central–Northeastern Tibet and the Tethyan Himalayas are tentatively compared to those of laboratory studies in order to infer constraints on the physical state of the Tibetan lower crust.

The P-wave velocity values in the lower crust resulting from arrival time and amplitude modelling appear to be low, 6.2–6.4 km/s in the north Qang Tang and 6.4–6.6 km/s in the Tethyan Himalayas, and slightly higher, 6.8–7.0 km/s in the north Bayan Har. A second observable is provided by the exceptional presence of S-waves reflected at the top and the bottom of the lower crust, not currently reported . It gives us strong direct constraints on velocity ratio values (Jiang et al., 2005—this issue). They appear significantly lower than the average value for a continental crust since we obtain values lower than 1.73 in all the sampled blocks.

Since these two parameters, P-wave velocity and P to S velocity ratio, are representative of the in situ composition, the different values we derived in the different blocks lead to the same conclusion of a lower crust with a composition from granitic to granodioritic (Sobolev and Babeyko, 1994; Christensen, 1996). Laboratory studies and whole rock models have derived relations between P-wave velocities and pressure and temperature (Sobolev and Babeyko, 1994). Combining P-wave velocities with the composition, that is granitic to granodioritic, we can deduce the temperature conditions of the lower crust of Tibet, given its pressure conditions, that is depth. In the P–T diagram, the north Qang Tang lower crust appear to have the highest temperature among the blocks we study, whereas the north Bayan Har has the lowest one (Fig. 4). In between these two ranges of temperature, is the lower crust of the Tethyan Himalayas due to its intermediate P-wave velocity. This means that at the crust–mantle boundary, at 75 km depth, temperatures in the north Qang Tang can be as high as 1100 °C whereas they are below 670 °C in the north Bayan Har and in the Tethyan Himalayas, they can reach a maximum of 985 °C.

Furthermore the refraction, wide-angle reflection waves, by their signal spectra and length of propagation in crustal layers is sensitive to a broad range of attenuation values. Comparing amplitudes of waves reflected at successive interfaces at depth, allows to use the amplitude loss on the difference in path to determine the quality factor Q that is to measure attenuation in the layer in-between, when the elastic model is reasonably constrained.

In northeastern Tibet, we do not find any evidence of a thick layer of partially molten material in the lower crust we sample, which is consistent with recording S Moho reflections while there were none in the Tethyan Himalayas. Furthermore the velocity models comprise low-velocity layers. These LVL cannot be due to partial melt since there would be very strong attenuation in correspondence, which is not observed.

They can thus be rather interpreted as due to anomalous superposition of material of contrasted lithologies resulting from tectonic evolution. This is in general agreement with the overriding of the northern edge of the Bayan Har crust over the Kun Lun crust and the imbrication of the southern edge of the Bayan Har into the crust of the Qang Tang, consistently with the crustal architecture derived by Jiang et al. (2005—this issue).

The lower crustal layer-average seismic quality factor Q, inverse attenuation of the medium is estimated from modelling the relative amplitudes of the wide-angle reflections at its bottom and top. Q cannot be lower than 2000 in the north Qang Tang where S-wave Moho reflections are also obtained. Q is bracketed by 1000 and 2000 in the north Bayan Har, where we observe Moho PmP reflected waves but no corresponding SmS waves. Q is 125 in the Tethyan Himalayas where S-wave deep crustal reflections are not observed and PmP has an amplitude several times smaller relative to that of the reflection on top the lower crust, and its spectrum has lost high frequencies (Sapin and Hirn, 1997).

Laboratory studies from Sato et al. have derived a relation between the quality factor Q and the ratio of the in situ temperature over the solidus temperature. Our previous estimate of the temperature in the lower crust of each terrane and this value of the homologous temperature derived from the estimate of Q allow us to deduce the solidus temperature relevant for the material sampled, i.e. to estimate the lower crust material is in the wet, dehydration or dry conditions.

Therefore, in the Qang Tang where the temperatures are the highest, the lower crustal material appear to be controlled by the dry conditions solidus. In the Bayan Har and the Tethyan Himalayas our data does not allow us to distinguish between two possibilities: the dehydration–melting solidus control the whole lower crustal layer, or the wet solidus control the top of the lower crust while its deeper part is depending on the dehydration–melting solidus.

Acknowledgments

This project was supported by the INSU-CNRS, the French Ministry of Research and Education, Paris, the French Embassy in Beijing and the Department of International Cooperation, Science Technology, Ministry of Land and Resources, Beijing. Discussions with Huang Chongli, Gao Ping and Chen Youfang are acknowledged. We also thank journal reviewers for their helpful suggestions to improve this paper.

References

Beck, S.L., Zandt, G., 2002. The nature of the orogenic crust in the central Andes. J. Geophys. Res. 107 (B10), 2230. doi:10.1029/2000JB000124.

Berckhemer, H., Kampfmann, W., Aulbach, E., Schmeling, H., 1982. Shear modulus and Q of forsterite and dunite near partial melting from forced-oscillation experiments. Phys. Earth Planet. Int. 29, 30–41.

Bird, P., Toksöz, M.N., 1977. Strong attenuation of Rayleigh waves in Tibet. Nature 266, 161–163.

Christensen, N.I., 1996. Poisson's ratio and crustal seismology. J. Geophys. Res. 101, 3139–3156.

Christensen, N.I., Mooney, W.D., 1995. Seismic velocity structure and composition of the continental crust: a global view. J. Geophys. Res. 100, 9761–9788.

Fuchs, K., Mueller, G., 1971. Computation of synthetic seismograms with the reflectivity method and comparison with observations. Geophys. J. R. Astron. Soc. 23, 417–433.

Fuchs, K., Schulz, K., 1976. Tunnelling of low-frequency waves through the subcrustal lithosphere. J. Geophys. 42, 175–190.

Galvé, A., Hirn, A., Jiang, M., Gallart, J., De Voogd, B., Lépine, J.-C., Diaz, J., Wang, Y., Qian, H., 2002a. Modes of raising northeastern Tibet probed by explosion seismology. Earth Planet. Sci. Lett. 203, 35–43.

Galvé, A., Sapin, M., Hirn, A., Diaz, J., Lépine, J.-C., Laigle, M., Gallart, J., Jiang, M., 2002b. Complex images of Moho and variation of V_p/V_s across the Himalaya and South Tibet, from a joint receiver-function and wide-angle-reflection approach. Geophys. Res. Lett. 29 (24), 2182. doi:10.1029/2002GL015611.

Hacker, B.R., Gnos, E., Ratschbacher, L., Grove, M., McWilliams, M., Sobolev, S.V., Jiang, W., Wu, Z., 2000. Hot and dry deep crustal xenoliths from Tibet. Science 287, 2463–2466.

Henry, P., Le Pichon, X., Goffé, B., 1997. Kinematic, thermal and petrological model of the Himalayas: constraints related to metamorphism within the underthrust Indian crust and topographic elevation. Tectonophysics 273, 31–56.

Hirn, A., Sapin, M., 1984. The Himalayan zone of crustal interaction: suggestions from explosion seismology. Ann. Geophys. 2, 123–130.

Hirn, A., Lépine, J.C., Jobert, G., Sapin, M., Wittlinger, G., Xu, Z.X., Gao, E.Y., Wang, X.J., Teng, J.W., Xiong, S.B., Pandey, M.R., Tater, J.M., 1984. Crustal structure and variability of the Himalayan boarder of Tibet. Nature 307, 23–25.

Hirn, A., Jiang, M., Sapin, M., Diaz, J., Nercessian, A., Lu, Q.T., Lépine, J.-C., Shi, D.N., Sachpazi, M., Pandey, M.R., Ma, K., Gallart, J., 1995. Seismic anisotropy as an indicator of mantle flow beneath the Himalayas and Tibet. Nature 375, 571–574.

Hirn, A., Sapin, M., Lépine, J.-C., Diaz, J., Jiang, M., 1997. Increase in melt fraction along a south–north traverse below the Tibetan plateau: evidence from seismology. Tectonophysics 273, 17–30.

Jackson, I., Paterson, M.S., Fitz Gerald, J.D., 1992. Seismic wave dispersion and attenuation in Aheim dunite: an experimental study. Geophys. J. Int. 108, 517–534.

xJiang, M., Galvé, A., Hirn, A., de Voogd, B., Laigle, M., Su, H.P., Diaz, J., Lépine, J.C., Wang, Y.X., 2005—this issue. Crustal thickening and variations in architecture from the Qaidam basin to the Qang Tang (north–central Tibetan plateau), from wide-angle reflection seismology. Tectonophysics 412, 121–140. doi:10.1016/j.tecto.2005.09.011.

Kampfmann, W., Berckhemer, H., 1985. High temperature experiments on the elastic and anelastic behaviour of magmatic rocks. Phys. Earth Planet. Inter. 40, 223–247.

Kapp, P., Yin, A., Manning, C.E., Harrison, T.M., Taylor, M.H., Ding, L., 2003. Tectonic evolution of the early Mesozoic blueschist-bearing Qiangtang metamorphic belt, central Tibet. Tectonics 22 (4), 1043. doi:10.1029/2002TC001383.

Kennett, B.L.N., 1975. The effect of attenuation on seismograms. Bull. Seismol. Soc. Am. 65, 1643–1653.

Le Pichon, X., Henry, P., Goffé, B., 1997. Uplift of Tibet: from eclogites to granulites—implications for the Andean Plateau and the Variscan belt. Tectonophysics 273, 57–76.

Makovsky, Y., Klemperer, S.L., 1999. Measuring the seismic properties of Tibetan bright spots: evidence for free aqueous fluids in the Tibetan middle crust. J. Geophys. Res. 104, 10795–10825.

Meissner, R.O., Vetter, U.R., 1970. Relationship between the seismic quality factor Q and the effective viscosity. J. Geophys. 45, 147–158.

Meissner, R., Tilmann, F., Haines, S., 2004. About the lithospheric structure of central Tibet, based on seismic data from the INDEPTH III profile. Tectonophysics 380, 1–25.

Min, Z., Wu, F.T., 1987. Nature of the upper crust beneath central Tibet. Earth Planet. Sci. Lett. 84, 204–210.

Owens, T.J., Zandt, G., 1997. Implications of crustal property variations for models of Tibetan plateau evolution. Nature 387, 37–43.

Pham, V.N., Boyer, D., Therme, P., Yuan, X.C., Li, L., Jin, G.Y., 1986. Partial melting zones in the crust in southern Tibet from magnetotelluric results. Nature 311, 310–314.

Sapin, M., Hirn, A., 1997. Seismic structure and evidence for eclogitization during the Himalayan convergence. Tectonophysics 273, 1–16.

Sapin, M., Wang, X.J., Hirn, A., Xu, Z.X., 1985. A seismic sounding in the crust of the Lhasa block, Tibet. Ann. Geophys. 3, 637–646.

Sato, H., 1991. Viscosity of the upper mantle from laboratory creep and anelasticity measurements in the peridotite at high pressure and temperature. Geophys. J. Int. 105, 587–599.

Sato, H., Manghnani, M.H., 1985. Ultrasonic measurements of V_p and Q_p: relaxation spectrum of complex modulus in basalt melts. Phys. Earth Planet. Inter. 41, 18–33.

Sato, H., Sacks, I.S., 1989. Anelasticity and thermal structure of the oceanic upper mantle: temperature calibration with heat flow data. J. Geophys. Res. 94, 5705–5715.

Sato, H., Sacks, I.S., Murase, T., 1989a. The use of laboratory velocity data for estimating temperature and partial melt fraction in the low-velocity zone: comparison with heat flow and electrical conductivity studies. J. Geophys. Res. 94, 5689–5704.

Sato, H., Sacks, I.S., Murase, T., Muncill, G., Fukuyama, H., 1989b. Q_p-melting temperature relation in peridotite at high pressure and temperature: attenuation mechanism and implications for the mechanical properties of the upper mantle. J. Geophys. Res. 94, 10647–10661.

Sherrington, H.F., Zandt, G., Frederiksen, A., 2004. Crustal fabric in the Tibetan plateau based on waveform inversions for seismic anisotropy parameters. J. Geophys. Res. 109, B02312. doi:10.1029/2002JB002345.

Sobolev, S.V., Babeyko, A.Y., 1994. Modeling of mineralogical composition, density and elastic wave velocities in anhydrous magmatic rocks. Surv. Geophys. 15, 515–544.

Vergne, J., Wittlinger, G., Qiang, H., Tapponnier, P., Poupinet, G., Jiang, M., Herquel, G., Paul, A., 2002. Seismic evidence for stepwise thickening of the crust across the north-eastern Tibetan plateau. Earth Planet. Sci. Lett. 203, 25–33.

Wei, W., Unsworth, M., Jones, A., Booker, J., Tan, H., Nelson, D., Chen, L., Li, S., Solon, K., Bedrosian, P., Jin, S., Deng, M., Ledo, J., Kay, D., Roberts, B., 2001. Detection of widespread fluids in the Tibetan crust by magnetotelluric studies. Science 292, 716–718.

Zandt, G., Ammon, C.J., 1995. Continental crust composition constrained by measurements of crustal Poisson's ratio. Nature 374, 152–154.